

See discussions, stats, and author profiles for this publication at: <https://www.researchgate.net/publication/267103221>

Gas Phase UV Spectrum of a Cu(II)–Bis(benzene) Sandwich Complex: Experiment and Theory

ARTICLE in THE JOURNAL OF PHYSICAL CHEMISTRY A · OCTOBER 2014

Impact Factor: 2.69 · DOI: 10.1021/jp506530g · Source: PubMed

READS

30

4 AUTHORS, INCLUDING:



Lifu Ma

University of Nottingham

9 PUBLICATIONS 35 CITATIONS

SEE PROFILE



Joseph K Koka

University of Nottingham

2 PUBLICATIONS 3 CITATIONS

SEE PROFILE



Hazel Cox

University of Sussex

38 PUBLICATIONS 521 CITATIONS

SEE PROFILE

1 Gas Phase UV Spectrum of a Cu(II)–Bis(benzene) Sandwich Complex: 2 Experiment and Theory

3 Lifu Ma, Joseph Koka, and Anthony J. Stace*

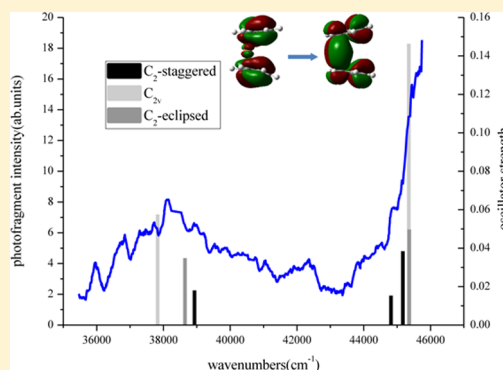
4 Department of Physical and Theoretical Chemistry, School of Chemistry, University of Nottingham, University Park, Nottingham
5 NG7 2RD, United Kingdom

Hazel Cox*

Department of Chemistry, University of Sussex, Falmer, Brighton BN1 9QJ, United Kingdom

6 Supporting Information

7 **ABSTRACT:** Photofragmentation with tunable UV radiation has been used
8 to generate a spectrum for the copper–bis(benzene) complex, $[\text{Cu}(\text{C}_6\text{H}_6)_2]^{2+}$, in the gas phase. The ions were held in an ion trap where
9 their temperature was reduced to ~ 150 K, whereby the spectrum revealed
10 two broad features at ~ 38200 and ~ 45700 cm^{-1} . Detailed calculations using
11 density functional theory (DFT) show the complex can occupy three
12 minimum energy structures with C_{2v} and C_2 (staggered and eclipsed)
13 symmetries. Adiabatic time-dependent DFT (TDDFT) has been used to
14 identify electronic transitions in $[\text{Cu}(\text{benzene})_2]^{2+}$, and the calculations
15 show these to fall into two groups that are in excellent agreement with the
16 experimental data. However, the open-shell electronic configuration of Cu^{2+}
17 (d^9) may give rise to excited states with double-excitation character, and the
18 single-excitation adiabatic TDDFT treatment leads to extensive spin
19 contamination. By quantifying the extent of spin contamination and allowing
20 for the inclusion of a small percentage ($\sim 10\%$), the theory can provide quantitative agreement with the experimental data.
21



22 ■ INTRODUCTION

23 Transition-metal-ion–benzene complexes have attracted atten-
24 tion because of their particular contribution to catalysis and
25 biological chemistry,¹ and numerous condensed phase studies
26 have been undertaken of the structure and reactivity of metal-
27 ion–bis (benzene) complexes.² Complementing this extensive
28 catalogue of work is the more limited study of metal-ion–
29 benzene complexes that can be prepared as stable species in the
30 gas phase. The advantages to come from such experiments are
31 that they can be performed on extremely small samples and
32 they avoid any perturbations that may come from solvent
33 molecules and/or counterions. These latter considerations are
34 of particular significance when it comes to recording spectra.
35 To date, most experiments on metal-ion–benzene complexes
36 have been undertaken on singly charged species, which are
37 comparatively easy to prepare and avoid any problems that may
38 arise from charge transfer, since very few metals have first
39 ionization energies that are higher than that of benzene.
40 However, if valid comparisons are to be made with their
41 condensed phase analogues, then it is important to develop
42 experimental methods that are capable of preparing metal-
43 benzene complexes where the metal occupies a more common
44 charge state [i.e., Fe(II), Cu(II), Ni(II), etc.]. In recent years
45 suitable techniques have appeared, and a wide range of
46 complexes containing first row transition metals in charge

states commonly observed in condensed phase chemistry have
47 been prepared and these include Mn(II),^{3,4} Co(II),⁵ Fe(II),^{6,7}
48 and Cu(II).^{8–17} These experiments are frequently done in
49 association with ligands that occupy pivotal positions in
50 traditional transition metal chemistry, such as H₂O, NH₃,
51 pyridine, and bipyridine.
52

The ability to generate metal-containing complexes with
53 sufficient signal strength for quantitative study (10^7 ions $\text{s}^{-1} \sim$
54 10^{-12} A) offers an opportunity to undertake a range of chemical
55 and physical measurements. To date, a number of research
56 groups have made important contributions to spectroscopic
57 studies of gas-phase transition metal complexes with benzene.
58 Duncan and co-workers have applied the IR-REMPI technique
59 to investigate a range of spectroscopic properties.^{18–24} Freiser
60 and co-workers have investigated photodissociation mecha-
61 nisms of Fe⁺, Co⁺, and Ni⁺ in association with benzene as a
62 function of radiation wavelength.²⁵ Yang and co-workers have
63 recorded spectra from group 6 metal (Cr, Mo, W) ion–bis
64 (benzene) sandwich complexes using the pulsed-field ionization
65 zero-electron kinetic energy (PFI-ZEKE) technique.²⁶ Rodgers
66 and co-workers have employed collision-induced dissociation
67

Received: July 1, 2014

Revised: October 19, 2014

(CID) measurements to examine the influence of d orbital occupation on the nature and strength of copper cation– π interactions,²⁷ and Armentrout and co-workers have investigated the binding energy between first-row transition metal ions (Ti^+ to Cu^+) and bis (benzene) by CID measurements.²⁸ In addition to this experimental progress, considerable computational effort has been devoted to calculating binding energies and exploring the nature of the bond between a transition metal ion and a benzene molecule. Bauschlicher et al. reported calculated binding energies for all first-row and selected second-row transition metal ions with benzene.²⁹ Numerous DFT studies on cationic, neutral, and anionic 3d transition metal ion–benzene half-sandwich and sandwich complexes have been reported,^{30–33} as have the results of calculations on yttrium and gadolinium bis(benzene) sandwich complexes.³⁴ Of the benzene complexes with first row transition metal, the bis (benzene) complex with Cu (II) is of particular interest because the d^9 electronic configuration provides the potential for structural distortion, and many of the issues surrounding this topic in Cu(II) complexes in general have been discussed in detail by Deeth et al.^{35–42} As an extension to the work discussed above on benzene complexes, Fan and co-workers have proposed a novel class of complex where a copper dimer is sandwiched between benzene molecules.⁴³ Previously, our work on metal dication d^9 complexes has combined experiment and theory in order to understand the origins of electronic transitions that have been observed at visible wavelengths in gas phase complexes of Cu(II) and Ag(II) with a variety of ligands.^{10,14,44} Although intended as studies of ligand field transitions, it was concluded from either recorded absorption cross sections or ion fragmentation patterns that most of these experiments have in fact involved charge transfer transitions. This paper presents new results from an experimental and theoretical study of the copper dication-bis(benzene) sandwich complex and, as such, represents the first investigation where the spectroscopy of a transition metal sandwich complex has been recorded for a metal ion in its most common charge state. To prepare the complex in the gas phase, use has been made of the pick-up technique and UV photofragmentation spectra have been recorded using a hybrid quadrupole ion trap instrument. The experimental UV spectra are discussed in conjunction with the results of DFT and TDDFT calculations in order to assign dominant electronic transitions appearing in the wavenumber range 35000–46000 cm^{-1} .

EXPERIMENT

A detailed description of the apparatus has been given elsewhere.⁴⁵ Briefly, argon carrier gas at a pressure of 2 bar has been passed through benzene held in an ice-cooled reservoir. The resultant mixed vapor was allowed to expand through a 50 μm diameter nozzle before passing through a 1 mm diameter skimmer. The collimated beam of mixed argon/solvent clusters then passed over a Knudsen cell containing pieces of copper heated to a temperature that was sufficient to generate metal vapor at a pressure of between 10^{-3} and 10^{-2} mbar. Under these conditions, a balance could be established between sufficient metal vapor for the effective pick up of atoms by the mixed clusters, the need to avoid scattering the molecular beam, and the contents of the crucible lasting the duration of a typical spectral scan (~ 45 h). To generate stable ion signals from the complex $[\text{Cu}(\text{benzene})_2]^{2+}$, the temper-

ature of the Knudsen cell was varied between 1340 and 1380 $^\circ\text{C}$.

Neutral copper/benzene complexes passed into the ion source of a quadrupole mass spectrometer (Extrel) where they were ionized by high-energy electron impact (100 eV). From a mixture of ions present in the source, the $[\text{Cu}(\text{benzene})_2]^{2+}$ complex was mass-selected with a quadrupole mass filter and steered by quadrupole deflector into an ion guide where it was transmitted to a quadrupole Paul ion trap. The end-cap electrodes of the latter were grounded and continuously cooled through a jacket that was attached to an external reservoir filled with liquid nitrogen. Helium buffer gas (5×10^{-4} mbar) contained within the trap was cooled by collisions with the cold surfaces, and over a total trapping time of 1.2 s, collisions between the helium atoms and trapped ions led to a considerable reduction in the internal energy content of the latter. On the basis of the observation of unimolecular decay by trapped ions, their internal temperature was thought to drop from >500 K to somewhere in the range of 100–150 K.^{45,46} Compared with previous examples of metal dication spectra,¹⁸ this cooling procedure has led to the appearance of discrete structure in spectra which, in turn, has made a valuable contribution to the assignment of transitions.^{4,47,48} The walls of the chamber housing the trap are baked continuously to reduce the water content of the background gas. In the absence of either an ion beam or buffer gas, the base pressure in the chamber was 2×10^{-8} mbar.

An electronic gate in front of the ion trap opened for 300 ms at the start of each trapping cycle and then shut for 900 ms to allow the ions to cool and undergo photoexcitation. The trapped ions were exposed to seven 10 ns pulses of tunable UV radiation from a frequency-doubled, Nd:YAG pumped dye laser. Subsequently, all precursor and photofragment ions were ejected from the trap by ramping the RF voltage on the ring electrode. A channeltron detector located behind one of the end-caps recorded ion signals, which were then averaged for 200 trap cycles, each lasting 1200 ms. An advantage of using the quadrupole trap is that ions with all values of m/z are swept out and detected at the end of each trap cycle. Spectra were calculated as

$$\text{photofragments yield} = \frac{\sum \text{photofragment intensities}}{\sum \text{photofragment intensities} + \sum \text{precursor ion intensity}} \quad (1)$$

and normalized with respect to variations in laser and precursor ion intensity.

THEORY

The structures and binding energies of $[\text{Cu}(\text{benzene})_2]^{2+}$ and $[\text{Cu}(\text{benzene})]^{+/2+}$ were calculated using density functional theory as implemented in GAUSSIAN 09.⁴⁹ Geometry optimizations and frequency analyses were performed using a range of functionals: BVP86,^{50,51} PBE,^{52,53} M06L,⁵⁴ B3LYP,⁵⁵ PBE0,^{52,56} M06,⁵⁷ and TPSSh.⁵⁸ In each case, structural minima were verified by the absence of imaginary vibrational modes. It was found that only PBE and PBE0 predicted three distinct minima, all other functionals predicted two of the three minima; however, there was good agreement on the energetic trends and reasonable to excellent agreement on key structural data where comparison was possible. The data obtained using PBE0 is presented here, and all other data can be found in the

Supporting Information. A 6-311++G(d,p) basis set was used for all atoms except Cu^{2+} , for which the standard SDD pseudopotential was used;^{59,60} this will be referred to as 6-311++G(d,p)[SDD] throughout the text. All energies presented are zero point energy corrected.

Excitation energies and oscillator strengths were calculated using adiabatic TDDFT with the optimized structures calculated using PBE0. The SCF step of TDDFT was performed using PBE0. The dominant transitions predicted by TDDFT were analyzed by calculating the natural transition orbitals (NTOs)⁶¹ in order to identify the contribution each orbital makes to an electronic transition.

RESULTS AND DISCUSSION

Experimental UV Photofragment Spectra. An example of a UV photofragment mass spectrum recorded from trapped $[\text{Cu}(\text{benzene})_2]^{2+}$ ion at 39500 cm^{-1} is shown in Figure 1.

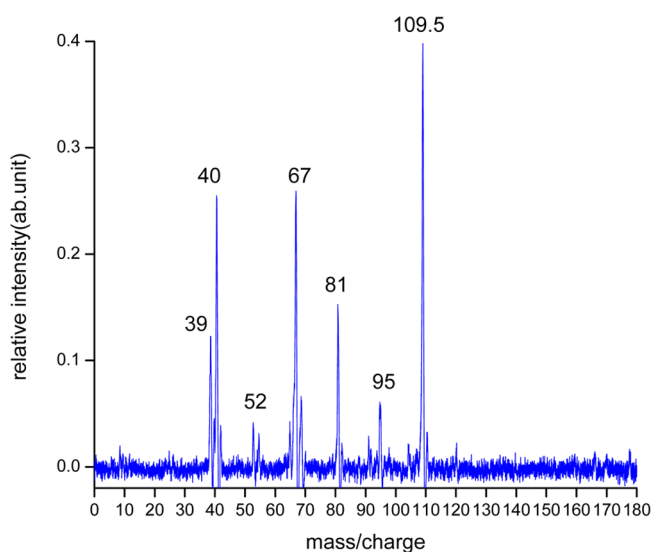


Figure 1. Example of a photofragment mass spectrum recorded for $[\text{Cu}(\text{benzene})_2]^{2+}$ in the UV at 39500 cm^{-1} .

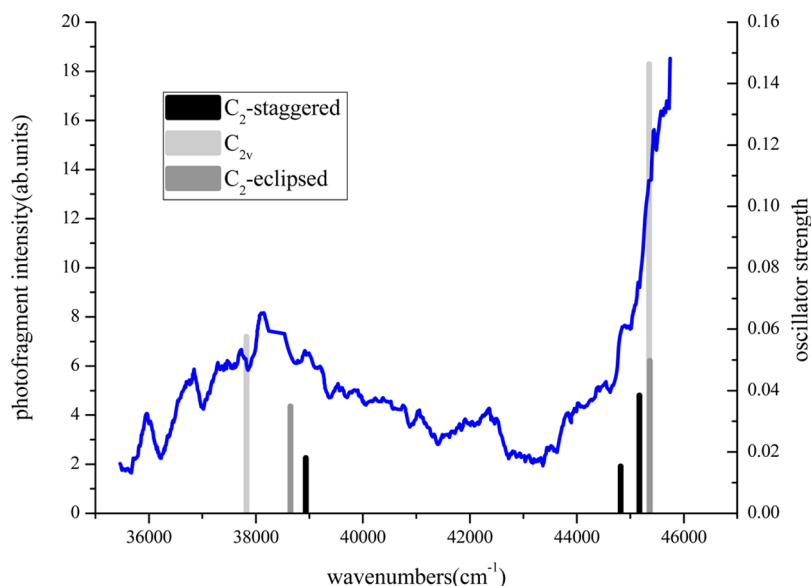
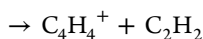
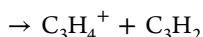
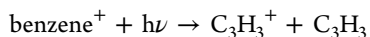
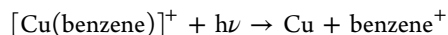
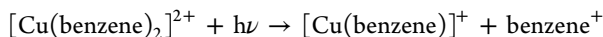


Figure 2. Experimental UV photofragment spectrum of $[\text{Cu}(\text{benzene})_2]^{2+}$ overlaid with calculated electronic transitions using TD-PBE0/6-311++G(d,p)[SDD] in conjunction with C_2 and C_{2v} geometries arising from PBE0/6-311++G(d,p)[SDD] geometry optimizations.

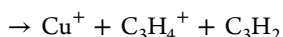
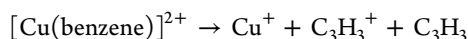
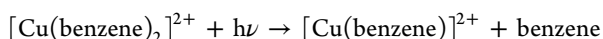
The parent ion $[\text{Cu}(\text{benzene})_2]^{2+}$ appears at 109.5 amu together with a wide range of ions at lower m/e values, which are assumed to be photofragments. Mass spectra recorded in the absence of laser radiation show the presence of background peaks at 67, 81, and 95 amu. In response to laser radiation, these particular ions exhibited a similar variation in intensity to the precursor ion, $[\text{Cu}(\text{benzene})_2]^{2+}$, therefore, they were included in with the latter for the purposes of determining the relative intensities of fragment ions. Tentative assignments for two of the ions are $\text{Cu}^+\text{H}_2\text{O}$ (81 amu) and Cu^+O_2 (95 amu); the ion at m/z 67 was the least sensitive to laser radiation and could be derived from a precursor that is coincident in mass with $[\text{Cu}(\text{benzene})_2]^{2+}$. The principal photofragments appear at 39, 40, and 52 amu and are thought to correspond to C_3H_3^+ , C_3H_4^+ , and C_4H_4^+ , which are fragment ions that have been seen following the photoexcitation of benzene.^{62–71}

In addition to contributions from $[\text{Cu}(\text{benzene})_2]^{2+}$, a complete analysis of the experimental spectra (see below) requires that possible contributions from $[\text{Cu}(\text{benzene})]^{+/2+}$ also be taken into account. However, previous experiments,¹⁰ had suggested that $[\text{Cu}(\text{benzene})]^{2+}$ is not stable. There is not an obvious mechanism that accounts for the photofragments observed for $[\text{Cu}(\text{benzene})_2]^{2+}$ since critical photofragments such as Cu^+ and benzene^+ are not observed. However, the dication complex decays with considerable excess energy as a result of charge transfer, which means that quite extensive fragmentation is possible. For the $\text{Cu}/\text{C}_6\text{H}_6$ system, the first and second ionization energies of copper are 7.88 and 20.29 eV, respectively; these numbers are to be compared with the first ionization energy of benzene, which is 9.42 eV. Therefore, charge transfer from Cu^{2+} to give Cu^+ and C_6H_6^+ would release a considerable amount of energy, some of which could easily lead to extensive fragmentation of the molecular ion. In an earlier study of $[\text{Pb}(\text{C}_6\text{H}_6)_2]^{2+}$, the only fragment observed as a result of photoexcitation was C_6H_6^+ .⁷² The absence of any metal-containing ion signal (e.g., Pb^+) was attributed to the possibility that a large release of kinetic energy to the fragments from Coulomb explosion could result in ions being ejected

from the trap. For a heavy metal ion, collisions with the helium buffer gas would not be sufficient to quench the ion's momentum. In addition, this earlier experiment provided evidence that fragment ions generated by the rapid decay of a precursor ion (<5 ns) were themselves subject to photofragmentation during the remainder of a photon pulse. Given the above considerations, the following are offered as possible photofragmentation mechanisms:



(1)



(2)

In mechanism (1), a benzene cation is produced by the photoinduced charge transfer of singly charged $[\text{Cu}(\text{benzene})]^+$.²⁷ The resultant benzene^+ is then photodissociated to give the observed fragment ions: C_3H_3^+ , C_3H_4^+ , or C_4H_4^+ .^{66,71} In mechanism (2), these same ions are generated as a result of charge transfer during the Coulomb fission of $[\text{Cu}(\text{benzene})]^{2+}$, where a possible energy difference of up to 10.87 eV would be sufficient to drive the appropriate reactions in C_6H_6^+ .

From the photofragment yields, a UV photofragment spectrum of $[\text{Cu}(\text{benzene})_2]^{2+}$ has been constructed by plotting the normalized ion intensity against photon wavenumber and these results are given in Figure 2. The spectrum can be seen to consist of two principal features: a moderately intense region centered at $\sim 38000 \text{ cm}^{-1}$ and a more intense feature that starts to rise at $\sim 43500 \text{ cm}^{-1}$ and extends beyond the upper wavenumber limit of the laser.

Calculated Structures and Binding Energies for $[\text{Cu}(\text{benzene})_2]^{2+}$. DFT calculations performed using PBE0/6-311++G(d,p)[SDD] predict three stable structures for the $[\text{Cu}(\text{benzene})_2]^{2+}$ complex, and these are shown in Figure 3; the energy difference between the three conformers is less than 25 kJ mol^{-1} . The highest energy structure has a bent C_{2v} geometry with eclipsed benzene rings. The bend angle, $\text{Bz}(\text{centroid})\text{--Cu--Bz}(\text{centroid}) = 133^\circ$ and the $\text{Bz}(\text{centroid})\text{--Cu}$ bond distance is 2.42 Å. A similar configuration has been identified in the optimized geometry of a copper-bis(phenalenyl) complex,⁷³ where a geometry with higher symmetry has been destabilized by a combination of Jahn–Teller distortion and the participation of d orbitals in σ bonding. The other two more stable structures are approximately parallel sandwich complexes with slipped rings in either an eclipsed or staggered configuration, with C_2 point group symmetry. The difference between the eclipsed and staggered conformers is less than 1 kJ mol^{-1} and the Bz--Cu--Bz bond angle and Bz--Cu bond distance are for the eclipsed structure:

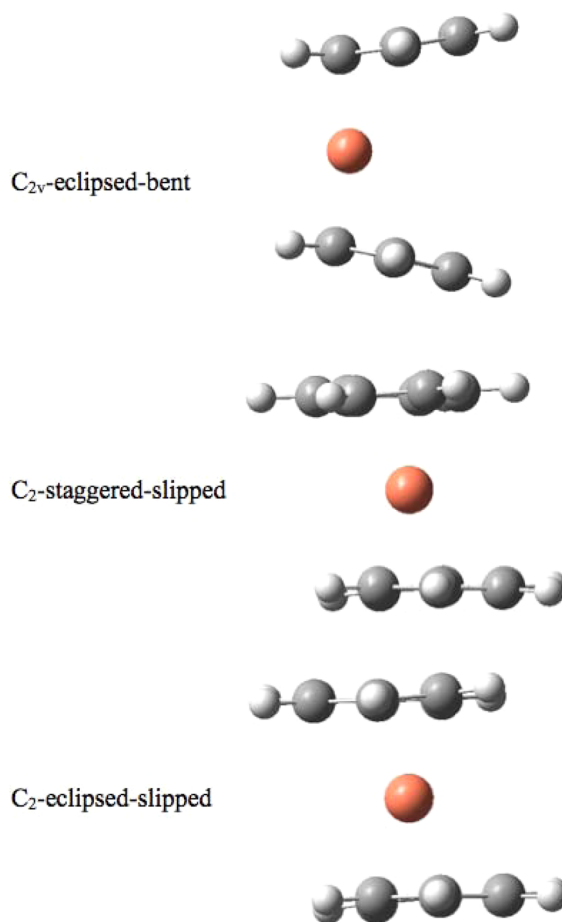


Figure 3. Optimized structures of $[\text{Cu}(\text{benzene})_2]^{2+}$ at the PBE0/6-311++G(d,p)[SDD] level of theory.

180° and 2.06 Å and for the staggered structure: 174° and 2.05 Å. In both cases (staggered and eclipsed), the structure has the metal localized over an η^3 site, which has been seen in previous calculations on $[\text{Cu}(\text{benzene})_2]^+$ and $[\text{Ni}(\text{benzene})_2]^{+2,74}$ and has been attributed to a pseudo Jahn–Teller distortion.^{38,40,75} Such a distortion is thought to arise from a mixing of the σ_u ligand-based HOMO with the π_g orbitals of the metal, resulting in new covalency, which stabilizes the configuration.⁷⁶

Calculations on $[\text{Cu}(\text{benzene})]^{+2+}$ were also performed at the same level of theory. $[\text{Cu}(\text{benzene})]^+$ has η^6 coordination with C_{6v} symmetry, while $[\text{Cu}(\text{benzene})]^{2+}$ has reduced symmetry due to the benzene ring having two carbon atoms distorted slightly toward the metal. Such a distortion has been observed in $[\text{Ni}(\text{benzene})]^+$ and other monocation–benzene complexes, and the results presented here support the observed trend that more strongly bound complexes favor distorted structures.⁷³

The binding energy of the dication complexes relative to complete neutral loss: $[\text{Cu}(\text{benzene})_2]^{2+} \rightarrow \text{Cu}^{2+} + 2 \text{ benzene}$, charge transfer: $[\text{Cu}(\text{benzene})_2]^{2+} \rightarrow [\text{Cu}(\text{benzene})]^+ + \text{benzene}^+$, and incremental neutral loss: $[\text{Cu}(\text{benzene})_2]^{2+} \rightarrow [\text{Cu}(\text{benzene})]^{2+} + \text{benzene}$ are given in Table 1. It can be seen that the binding energy of the complex relative to the incremental neutral ligand loss asymptote is substantial ($>300 \text{ kJ mol}^{-1}$) but that the complex is metastable with respect to charge transfer as the lowest energy asymptote corresponding to charge transfer lies below the bound state. It is clear from Table 1 that the binding energies for the different conformers 315

Table 1. Calculated Binding Energies (kJ mol⁻¹) at the PBE0/6-311++G(d,p)[SDD] Level of Theory for the [Cu(benzene)₂]²⁺ Complex with Respect to the Formation of a Range of Products^a

reaction	geometry	binding energy (kJ mol ⁻¹)
[Cu(benzene) ₂] ²⁺ → Cu ²⁺ + 2 benzene	C _{2v}	1158.8
	C _{2v} -staggered	1182.0
	C _{2v} -eclipsed	1182.2
[Cu(benzene) ₂] ²⁺ → [Cu(benzene)] ⁺ + benzene ⁺	C _{2v}	-164.5
	C _{2v} -staggered	-141.4
	C _{2v} -eclipsed	-141.2
[Cu(benzene) ₂] ²⁺ → [Cu(benzene)] ²⁺ + benzene	C _{2v}	325.2
	C _{2v} -staggered	348.3
	C _{2v} -eclipsed	348.5

^aA negative value indicates the zero-point energy corrected reaction energy is exothermic.

Table 2. Summary of Observed and Calculated TDDFT Electronic Transitions and Oscillator Strengths ($f \geq 0.01$ in the Experimental Range of 35000–46000 cm⁻¹) for [Cu(benzene)₂]²⁺ Using TD-PBE0/6-311++G(d,p)[SDD]^a

peak positions (cm ⁻¹)				$\langle \hat{S}^2 \rangle$	assignment ^c (based on NTO description)
observed	calculated	f			
38200	37824 ^b	0.0575	1.027		L(ML)CT $\pi \rightarrow (10\% \text{Cu})4p + \pi^e$
	38646 ^d	0.0347	1.806		(ML)(ML)CT (12% Cu) 3s + (12% Cu) 3d + $\pi \rightarrow 4p$ (30% Cu) + π^e
	38933 ^c	0.018	1.85		ligand based electronic transition $\pi \rightarrow \pi^e$
~45700	44819 ^c	0.0153	1.05		(ML)LCT 3d(19%Cu) + $\pi \rightarrow \pi^e$
	45171 ^c	0.0384	1.091		(ML)LCT 3d(19%Cu) + $\pi \rightarrow \pi^e$
	45352 ^b	0.1463	1.127		L(ML)CT $\pi \rightarrow (15\% \text{Cu})4s + \pi^e$
	45364 ^d	0.0497	1.082		(ML)LCT (18% Cu) 3d + (12% Cu) 3s + $\pi \rightarrow \pi^e$

^aThe weight and character of the dominant configuration for the alpha spin, and the % Cu character, is also provided. See text for a discussion of $\langle \hat{S}^2 \rangle$, which should be 0.75 in the absence of spin contamination. ^bC_{2v}-eclipsed. ^cC_{2v}-staggered. ^dC_{2v}-eclipsed. ^eLess than 60% metal character is (arbitrarily) classed as a metal–ligand (ML) orbital rather than a metal (M) orbital.

differ by less than 25 kJ mol⁻¹. When compared with the energy available at the point of ion formation in the experiment, the comparatively small energy differences shown in Table 1 mean that, in order to fully assign the spectra, all conformers should be considered in the TDDFT calculations.

TDDFT Calculation of Spectra. Excitation energies and oscillator strengths of the optimized structures of the [Cu(benzene)₂]²⁺ complex with C_{2v}, C₂ (staggered), and C₂ (eclipsed) conformations were calculated at the TD-PBE0/6-311++G(d,p)[SDD] level of theory. The calculated TDDFT excitations in the experimental range are presented as stick spectra in Figure 2 together with a complete experimental UV photofragment spectrum. The dominant electronic transitions (oscillator strength, $f \geq 0.01$), and assignments, based on the NTO contributions involved in each transition, are provided in Table 2. From Figure 2, it can be seen that all of the calculated excitations arising from the three geometries fall into two groups under the two broad structures at ~38200 and ~45700 cm⁻¹ in the experimental spectrum. Overall, the agreement between the regions where the calculated transitions fall and the broad experimental features is excellent.

In Table 2, the excitations are assigned according to their nature, which has been identified from the natural transition orbitals involved in the movement of electron population. A ligand-to-metal ligand (ML) charge transfer at 37824 cm⁻¹, a metal ligand-to-metal ligand at 38646 cm⁻¹, and a ligand-based $\pi \rightarrow \pi^*$ excitation at 38933 cm⁻¹ can be matched to the feature at approximately 38200 cm⁻¹. A separate group of charge transfer transitions (CT) in the form of (ML)LCT transitions and a L(ML)CT transitions in the range 44500–45500 cm⁻¹ can be assigned to the broad feature which starts at ~44500 cm⁻¹. Comparing Figure 2 and Table 2, it can be seen that the L(ML)CT transitions arise from the C_{2v}-eclipsed conformer, the (ML)LCT and (ML)(ML)CT transitions arise from the C₂-eclipsed conformer, and the ligand-based and (ML)LCT transitions arise from the C₂-staggered conformer.

To explore other possible contributions to the experimental spectrum, excitation energies and oscillator strengths were also calculated for the [Cu(benzene)]^{+/2+} complexes at the TD-PBE0/6-311++G(d,p)[SDD] level of theory. For both systems,

only one excitation (with $f \geq 0.01$) appeared within the profile of the experimental spectrum: at approximately 44200 cm⁻¹ for [Cu(benzene)]⁺ and 44800 cm⁻¹ for [Cu(benzene)]²⁺. However, the latter ion has not been observed in these or other experiments that have investigated Cu²⁺–benzene complexes.

Spin Contamination in Open-Shell Excited States. Adiabatic TDDFT appears capable of predicting electronic transitions in those regions of the UV where the experiment has shown spectral features to be present for [Cu(benzene)₂]²⁺. However, one topic has not been addressed and that is spin contamination and the extent to which it influences the validity of excitations that have been calculated for the open-shell complexes [Cu(benzene)₂]²⁺ and [Cu(benzene)]²⁺.

The level of spin contamination provides an indication of the degree of unphysical and/or missing states in the calculated spectrum due to the absence of double-excitations, which need to be correctly described for some spin-adapted configurations arising from a d⁹ system with a doublet ground state. A measure of spin contamination is provided by the extent to which the calculated $\langle \hat{S}^2 \rangle$ value differs from the value expected from the same operator for a doublet state, which is 0.75.^{72,77} Assuming that quartet states ($\langle \hat{S}^2 \rangle = 3.75$) constitute the primary source of contamination in these dications, that is,

$$|\text{Cu(benzene)}_2^{2+}\rangle = C_D|\text{doublet}\rangle + C_Q|\text{quartet}\rangle \langle \hat{S}^2_{\text{calc}} \rangle = 0.75|C_D|^2 + 3.75|C_Q|^2$$

The percentage of doublet character in the Kohn–Sham wave function for each of the open-shell excited states can then be calculated and is given in Table 3. From these results, it can be seen that all of the calculated excitations suffer from some degree of spin contamination (i.e., $\Delta\langle \hat{S}^2 \rangle = \langle \hat{S}^2 \rangle - 0.75 \neq 0$). Those with high $\Delta\langle \hat{S}^2 \rangle$ values should be discarded; however, there are two transitions appearing at 37824 and 44819 cm⁻¹,

Table 3. Spin Contamination in Each of the $[\text{Cu}(\text{benzene})_2]^{2+}$ and $[\text{Cu}(\text{benzene})]^{2+}$ Excited States Calculated Using TD-PBE0/6-311++G(d,p)[SDD] and Assuming that All Spin Contamination Comes from the Next Highest Allowed Spin Component

complex	$E \text{ (cm}^{-1}\text{)}$	$\langle \hat{S}^2 \rangle$	$\Delta \langle \hat{S}^2 \rangle$	doublet character (%)	spin contamination (%)
$[\text{Cu}(\text{benzene})_2]^{2+}$	37824 ^a	1.03 ^a	0.28 ^a	90.8 ^a	9.2 ^a
	38646	1.81	1.06	64.8	35.2
	38933	1.85	1.10	63.3	36.7
	44819 ^a	1.05 ^a	0.30 ^a	90.0 ^a	10.0 ^a
	45171 ^a	1.09 ^a	0.34 ^a	88.6 ^a	11.4 ^a
	45352 ^a	1.13 ^a	0.38 ^a	87.4 ^a	12.6 ^a
	45364 ^a	1.08 ^a	0.33 ^a	88.9 ^a	11.1 ^a
	44415	1.27	0.52	82.6	17.4
$[\text{Cu}(\text{benzene})]^{2+}$	44827	1.28	0.53	82.4	17.6

^aThe states that are least affected by spin contamination.

where $\Delta \langle \hat{S}^2 \rangle \leq 0.3$, and there are three more where $\Delta \langle \hat{S}^2 \rangle \approx 0.35$. Assuming that the dominant contribution to spin contamination comes from the next highest spin component, these excited states have approximately 90% doublet character, in which case these excitations are highly likely to occur and, as noted earlier, they fall within the profile of the experimental spectrum. Obviously, any transitions calculated for $[\text{Cu}(\text{benzene})]^{2+}$ are not subject to spin contamination.

CONCLUSION

A UV photofragmentation spectrum has been recorded for $[\text{Cu}(\text{benzene})_2]^{2+}$ in the gas phase using a quadrupole ion trap mass spectrometer and where C_3H_3^+ , C_3H_4^+ , and C_4H_4^+ have been identified as photofragments. DFT structures with C_2 and C_{2v} symmetries have been confirmed as minima and adiabatic TDDFT has been used to identify a range of electronic transitions in $[\text{Cu}(\text{benzene})_2]^{2+}$ which involve electron displacements of the form $\pi \rightarrow \text{Cu}$, $\text{Cu} \rightarrow \pi^*$, and $\pi \rightarrow \pi^*$. When spin contamination is taken into consideration, there are at least four electronic transitions that can be assigned to the experimental spectrum.

ASSOCIATED CONTENT

Supporting Information

Functional comparison of optimized geometries: relative energies and key structural parameters for $[\text{Cu}(\text{benzene})_2]^{2+}$; Cartesian coordinates for all stationary points calculated at the PBE0/6-311++G(d,p)[SDD] level of theory. This material is available free of charge via the Internet at <http://pubs.acs.org>.

AUTHOR INFORMATION

Corresponding Authors

*E-mail: a.j.stace@nottingham.ac.uk.*E-mail: h.cox@sussex.ac.uk.

Notes

The authors declare no competing financial interest.

ACKNOWLEDGMENTS

H.C. and L.M. would like to acknowledge the use of the EPSRC UK National Service for Computational Chemistry Software (NSCCS) at Imperial College London in carrying out this work. L.M. and J.K. would like to thank the University of Nottingham for the award of scholarships and for financial support for the experimental work. The authors are grateful to Prof. R. Deeth for his critical reading of the manuscript.

REFERENCES

- (1) Dougherty, D. A. Cation- π Interactions in Chemistry and Biology: A New View of Benzene, Phe, Tyr, and Trp. *Science* (Washington, D.C.) **1996**, 271, 163–168.
- (2) Muetterties, E. L.; Bleeke, J. R.; Wucherer, E. J.; Albright, T. Structural, Stereochemical, and Electronic Features of Arene-Metal Complexes. *Chem. Rev.* **1982**, 82, 499–525.
- (3) Cox, H.; Akibo-Betts, G.; Wright, R. R.; Walker, N. R.; Curtis, S.; Duncombe, B.; Stace, A. J. Solvent Coordination in Gas-Phase $[\text{Mn}(\text{H}_2\text{O})_N]^{2+}$ and $[\text{Mn}(\text{ROH})_N]^{2+}$ Complexes: Theory and Experiment. *J. Am. Chem. Soc.* **2003**, 125, 233–242.
- (4) Wu, G.; Stewart, H.; Lemon, F. D.; Cox, H.; Stace, A. J. The UV Photofragmentation Spectroscopy of the Metal Dication Complex $[\text{Mn}(\text{Pyridine})_4]^{2+}$. *Mol. Phys.* **2010**, 108, 1199–1208.
- (5) Kohler, M.; Leary, J. A. Gas-Phase Reactions of Doubly Charged Alkaline Earth and Transition Metal Complexes of Acetonitrile, Pyridine, and Methanol Generated by Electrospray Ionization. *J. Am. Soc. Mass Spectrom.* **1997**, 8, 1124–1133.
- (6) Blades, A. T.; Jayaweera, P.; Ikononou, M. G.; Kebarle, P. Ion-Molecule Clusters Involving Doubly Charged Metal Ions (M^{2+}). *Int. J. Mass Spectrom. Ion Processes* **1990**, 102, 251–67.
- (7) Spence, T. G.; Trotter, B. T.; Posey, L. A. Influence of Sequential Solvation on Metal-to-Ligand Charge Transfer in Bis(2,2',2''-Terpyridyl)Iron(II) Clustered with Dimethyl Sulfoxide. *J. Phys. Chem. A* **1998**, 102, 7779–7786.
- (8) Puskar, L.; Stace, A. J. UV Photofragmentation of Gas Phase M^+ and M^{2+} Complexes with Ketones, Where $\text{M} = \text{Cu}$ and Ag . *Mol. Phys.* **2005**, 103, 1829–1835.
- (9) Duncombe, B. J.; Duale, K.; Buchanan-Smith, A.; Stace, A. J. The Solvation of Cu^{2+} with Gas-Phase Clusters of Water and Ammonia. *J. Phys. Chem. A* **2007**, 111, 5158–5165.
- (10) Puskar, L.; Cox, H.; Goren, A.; Aitken, G. D. C.; Stace, A. J. Ligand Field Spectroscopy of $\text{Cu}(\text{II})$ and $\text{Ag}(\text{II})$ Complexes in the Gas Phase: Theory and Experiment. *Faraday Discuss.* **2003**, 124, 259–273.
- (11) Wright, R. R.; Walker, N. R.; Firth, S.; Stace, A. J. Coordination and Chemistry of Stable $\text{Cu}(\text{II})$ Complexes in the Gas Phase. *J. Phys. Chem. A* **2001**, 105, 54–64.
- (12) Walker, N. R.; Wright, R. R.; Barran, P. E.; Cox, H.; Stace, A. J. Unexpected Stability of $[\text{CuAr}]^{2+}$, $[\text{AgAr}]^{2+}$, $[\text{AuAr}]^{2+}$, and Their Larger Clusters. *J. Chem. Phys.* **2001**, 114, 5562–5567.
- (13) Walker, N. R.; Wright, R. R.; Barran, P. E.; Murrell, J. N.; Stace, A. J. Comparisons in the Behavior of Stable Copper(II), Silver(II), and Gold(II) Complexes in the Gas Phase: Are There Implications for Condensed-Phase Chemistry? *J. Am. Chem. Soc.* **2001**, 123, 4223–4227.
- (14) Puskar, L.; Stace, A. J. Gas Phase Ligand Field Photofragmentation Spectroscopy. *J. Chem. Phys.* **2001**, 114, 6499–6501.
- (15) Puskar, L.; Barran, P. E.; Wright, R. R.; Kirkwood, D. A.; Stace, A. J. The Ultraviolet Photofragmentation of Doubly Charged Transition Metal Complexes in the Gas Phase: Initial Results for $[\text{Cu}(\text{Pyridine})_N]^{2+}$ and $[\text{Ag}(\text{Pyridine})_N]^{2+}$ Ions. *J. Chem. Phys.* **2000**, 112, 7751–7754.

- (16) Walker, N. R.; Firth, S.; Stace, A. J. Stable Cu(II) Coordination Complexes in the Gas Phase. *Chem. Phys. Lett.* **1998**, *292*, 125–132.
- (17) Stace, A. J.; Walker, N. R.; Firth, S. $[\text{Cu}(\text{H}_2\text{O})_N]^{2+}$ Clusters: The First Evidence of Aqueous Cu(II) in the Gas Phase. *J. Am. Chem. Soc.* **1997**, *119*, 10239–10240.
- (18) van, H. D.; von, H. G.; Meijer, G.; Maitre, P.; Duncan, M. A. Infrared Spectra of Gas-Phase $\text{V}^+(\text{Benzene})$ and $\text{V}^+(\text{Benzene})_2$ Complexes. *J. Am. Chem. Soc.* **2002**, *124*, 1562–1563.
- (19) Jaeger, T. D.; Duncan, M. A. Photodissociation of $\text{M}^+(\text{Benzene})_X$ Complexes ($\text{M} = \text{Ti}, \text{V}, \text{Ni}$) at 355 nm. *Int. J. Mass Spectrom.* **2005**, *241*, 165–171.
- (20) Jaeger, T. D.; Duncan, M. A. Vibrational Spectroscopy of $\text{Ni}^+(\text{Benzene})_N$ Complexes in the Gas Phase. *J. Phys. Chem. A* **2005**, *109*, 3311–3317.
- (21) Jaeger, T. D.; Van, H. D.; Klippenstein, S. J.; Von, H. G.; Meijer, G.; Duncan, M. A. Vibrational Spectroscopy and Density Functional Theory of Transition-Metal Ion-Benzene and Dibenzene Complexes in the Gas Phase. *J. Am. Chem. Soc.* **2004**, *126*, 10981–10991.
- (22) Jaeger, T. D.; Pillai, E. D.; Duncan, M. A. Structure, Coordination, and Solvation of $\text{V}^+(\text{Benzene})_N$ Complexes Via Gas Phase Infrared Spectroscopy. *J. Phys. Chem. A* **2004**, *108*, 6605–6610.
- (23) Willey, K. F.; Yeh, C. S.; Robbins, D. L.; Pilgrim, J. S.; Duncan, M. A. Photodissociation Spectroscopy of Aquamagnesium(1+) and Aqua-D2-Magnesium(1+) ($\text{Mg}^+-\text{H}_2\text{O}$ and $\text{Mg}^+-\text{D}_2\text{O}$). *J. Chem. Phys.* **1992**, *97*, 8886–8895.
- (24) Willey, K. F.; Cheng, P. Y.; Yeh, C. S.; Robbins, D. L.; Duncan, M. A. Electronic Spectroscopy of Silver Dimer-Rare Gas Complexes. *J. Chem. Phys.* **1991**, *95*, 6249–6256.
- (25) Hettich, R. L.; Jackson, T. C.; Stanko, E. M.; Freiser, B. S. Gas-Phase Photodissociation of Organometallic Ions. Bond Energy and Structure Determinations. *J. Am. Chem. Soc.* **1986**, *108*, 5086–5093.
- (26) Sohnlein, B. R.; Yang, D.-S. Pulsed-Field Ionization Electron Spectroscopy of Group 6 Metal (Cr, Mo, and W) Bis(Benzene) Sandwich Complexes. *J. Chem. Phys.* **2006**, *124*, 134305/1–134305/8.
- (27) Ruan, C.; Yang, Z.; Rodgers, M. T. Influence of the D Orbital Occupation on the Nature and Strength of Copper Cation-II Interactions: Threshold Collision-Induced Dissociation and Theoretical Studies. *Phys. Chem. Chem. Phys.* **2007**, *9*, 5902–5918.
- (28) Meyer, F.; Khan, F. A.; Armentrout, P. B. Thermochemistry of Transition Metal Benzene Complexes: Binding Energies of $\text{M}(\text{C}_6\text{H}_6)_X^+$ ($X = 1, 2$) for $\text{M} = \text{Ti}$ to Cu . *J. Am. Chem. Soc.* **1995**, *117*, 9740–9748.
- (29) Bauschlicher, C. W., Jr.; Sodupe, M.; Partridge, H. A Theoretical Study of the Positive and Dipositive Ions of Alkaline Earth(M) Ammine and Aqua Complexes ($\text{M}(\text{NH}_3)_N$ and $\text{M}(\text{H}_2\text{O})_N$) for $\text{M} = \text{Magnesium}, \text{Calcium}, \text{or Strontium}$. *J. Chem. Phys.* **1992**, *96*, 4453–63.
- (30) Wedderburn, K. M.; Bililign, S.; Levy, M.; Gdanitz, R. J. Geometries and Stabilities of 3d-Transition Metal-Cation Benzene Complexes, M^+Bz_N ($\text{M} = \text{Sc-Cu}$, $N = 1, 2$). *Chem. Phys.* **2006**, *326*, 600–604.
- (31) Kandam, A. K.; Rao, B. K.; Jena, P.; Pandey, R. Geometry and Electronic Structure of $\text{V}_n(\text{Bz})_M$ Complexes. *J. Chem. Phys.* **2004**, *120*, 10414–10422.
- (32) Pandey, R.; Rao, B. K.; Jena, P.; Blanco, M. A. Electronic Structure and Properties of Transition Metal-Benzene Complexes. *J. Am. Chem. Soc.* **2001**, *123*, 3799–808.
- (33) Pandey, R.; Rao, B. K.; Jena, P.; Newsam, J. M. Unique Magnetic Signature of Transition Metal Atoms Supported on Benzene. *Chem. Phys. Lett.* **2000**, *321*, 142–150.
- (34) Di, B. S.; Lanza, G.; Fraga, I. L.; Marks, T. J. Electronic Structure, Molecular Geometry, and Bonding Energetics in Zero-Valent Yttrium and Gadolinium Bis(Arene) Sandwich Complexes. A Theoretical Ab Initio Study. *Organometallics* **1996**, *15*, 3985–3989.
- (35) Deeth, R. J.; Paget, V. J. Molecular Mechanics Calculations on Imine and Mixed-Ligand Systems of CoII, NiII and CuII. *J. Chem. Soc., Dalton Trans.* **1997**, 537–546.
- (36) Davies, I. W.; Deeth, R. J.; Larsen, R. D.; Reider, P. J. A Clfse/Mm Study on the Role of Ligand Bite-Angle in Cu(II)-Catalyzed Diels-Alder Reactions. *Tetrahedron Lett.* **1999**, *40*, 1233–1236.
- (37) Burton, V. J.; Deeth, R. J. Molecular Modeling for Copper(II) Centers. *J. Chem. Soc., Chem. Commun.* **1995**, 573–574.
- (38) Deeth, R. J. A Combined Ligand Field and Density Functional Theory Study of the Structural and Spectroscopic Properties of $[\text{Cu}(\text{Dien})_2]^{2+}$. *J. Chem. Soc., Dalton Trans.* **2001**, 664–669.
- (39) Deeth, R. J.; Hearnshaw, L. J. A. Molecular Modelling for Coordination Compounds: Cu(II)-Amine Complexes. *Dalton Trans.* **2005**, 3638–3645.
- (40) Deeth, R. J.; Hitchman, M. A. Factors Influencing Jahn-Teller Distortions in Six-Coordinate Copper(II) and Low-Spin Nickel(II) Complexes. *Inorg. Chem.* **1986**, *25*, 1225–1233.
- (41) Deeth, R. J. Impact on Ligand-Field Theory of the Real Ground State for Copper Dichloride. *J. Chem. Soc., Dalton Trans.* **1993**, 1061–1064.
- (42) Bentz, A.; Comba, P.; Deeth, R. J.; Kersch, M.; Seibold, B.; Wadepohl, H. Modeling of the Various Minima on the Potential Energy Surface of Bispidine Copper(II) Complexes: A Further Test for Ligand Field Molecular Mechanics. *Inorg. Chem.* **2008**, *47*, 9518–9527.
- (43) Zhou, J.; Wang, W.-N.; Fan, K.-N. Novel Compounds with Cobalt, Copper, and Nickel Dimers Sandwiched between Benzene Molecules: A DFT Study. *Chem. Phys. Lett.* **2006**, *424*, 247–251.
- (44) Guan, J.; Puskar, L.; Esplugas, R. O.; Cox, H.; Stace, A. J. Ligand Field Photofragmentation Spectroscopy of $[\text{Ag}(\text{L})_N]^{2+}$ Complexes in the Gas Phase: Experiment and Theory. *J. Chem. Phys.* **2007**, *127*, 064311/1–064311/12.
- (45) Wu, G.; Chapman, D.; Stace, A. J. Trapping and Recording the Collision- and Photoinduced Fragmentation Patterns of Multiply Charged Metal Complexes in the Gas Phase. *Int. J. Mass Spectrom.* **2007**, *262*, 211–219.
- (46) Wu, G.; Guan, J.; Aitken, G. D. C.; Cox, H.; Stace, A. J. Infrared Multiphoton Spectra from Metal Dication Complexes in the Gas Phase. *J. Chem. Phys.* **2006**, *124*, 201103/1–201103/4.
- (47) Wu, G.; Norris, C.; Stewart, H.; Cox, H.; Stace, A. J. State-Resolved UV Photofragmentation Spectrum of the Metal Dication Complex $[\text{Zn}(\text{Pyridine})_4]^{2+}$. *Chem. Commun. (Cambridge, U.K.)* **2008**, 4153–4155.
- (48) Stewart, H.; Wu, G.; Ma, L.; Barclay, M.; Vieira, A. D.; King, A.; Cox, H.; Stace, A. J. Ultraviolet Photofragmentation Spectroscopy of Alkaline Earth Dication Complexes with Pyridine and 4-Picoline (4-Methyl Pyridine). *J. Phys. Chem. A* **2011**, *115*, 6948–6960.
- (49) Frisch, M. J.; Trucks, G. W.; Schlegel, H. B.; Scuseria, G. E.; Robb, M. A.; Cheeseman, J. R.; Scalmani, G.; Barone, V.; Mennucci, B.; Petersson, G. A., et al., *Gaussian 09*, revision A.02, Gaussian, Inc.: Wallingford, CT, 2009.
- (50) Becke, A. D. Density-Functional Exchange-Energy Approximation with Correct Asymptotic-Behavior. *Phys. Rev. A* **1998**, *38*, 3098–3100.
- (51) Perdew, J. P. Density-Functional Approximation for the Correlation Energy of the Inhomogeneous Electron Gas. *Phys. Rev. B* **1986**, *33*, 8822–8824.
- (52) Perdew, J. P.; Burke, K.; Ernzerhof, M. Generalized Gradient Approximation Made Simple. *Phys. Rev. Lett.* **1996**, *77*, 3865–3868.
- (53) Perdew, J. P.; Burke, K.; Ernzerhof, M. Errata: Generalized Gradient Approximation Made Simple. *Phys. Rev. Lett.* **1997**, *78*, 1396.
- (54) Zhao, Y.; Truhlar, D. G. A New Local Density Functional for Main-Group Thermochemistry, Transition Metal Bonding, Thermochemical Kinetics, and Noncovalent Interactions. *J. Chem. Phys.* **2006**, *125*, 194101/1–194101/18.
- (55) Becke, A. D. Density-Functional Exchange-Energy Approximation with Correct Asymptotic Behavior. *Phys. Rev. A* **1988**, *38*, 3098–3100.
- (56) Adamo, C.; Barone, V. Toward Reliable Density Functional Methods without Adjustable Parameters: The PBE0 Model. *J. Chem. Phys.* **1999**, *110*, 6158–6170.
- (57) Zhao, Y.; Truhlar, D. G. The M06 Suite of Density Functionals for Main Group Thermochemistry, Thermochemical Kinetics, Noncovalent Interactions, Excited States, and Transition Elements: Two New Functionals and Systematic Testing of Four M06-Class 617

- 618 Functionals and 12 Other Functionals. *Theor. Chem. Acc.* **2008**, *120*,
619 215–241.
- 620 (58) Tao, J.; Perdew, J. P.; Staroverov, V. N.; Scuseria, G. E.
621 Climbing the Density Functional Ladder: Nonempirical Meta-
622 Generalized Gradient Approximation Designed for Molecules and
623 Solids. *Phys. Rev. Lett.* **2003**, *91*, 146401/1–146401/4.
- 624 (59) Institut für Theoretische Chemie [http://www.theochem.uni-](http://www.theochem.uni-stuttgart.de)
625 [stuttgart.de](http://www.theochem.uni-stuttgart.de) (accessed Oct 25, 2014).
- 626 (60) Kuechle, W.; Dolg, M.; Stoll, H.; Preuss, H. Ab Initio
627 Pseudopotentials for Mercury through Radon. I. Parameter Sets and
628 Atomic Calculations. *Mol. Phys.* **1991**, *74*, 1245–63.
- 629 (61) Martin, R. L. Natural Transition Orbitals. *J. Chem. Phys.* **2003**,
630 *118*, 4775–4777.
- 631 (62) Sedgwick, J. B.; Nelson, P. R.; Steiner, P. A.; Moran, T. F.
632 Charge Neutralization of Ions from Benzene. *Org. Mass Spectrom.*
633 **1988**, *23*, 256–260.
- 634 (63) Yokoyama, A.; Zhao, X.; Hints, E. J.; Continetti, R. E.; Lee, Y.
635 T. Molecular Beam Studies of the Photodissociation of Benzene at 193
636 and 248 nm. *J. Chem. Phys.* **1990**, *92*, 4222–4233.
- 637 (64) Eland, J. H. D.; Schulte, H. Unimolecular Ion Decompositions:
638 Rate Constants as a Function of Excitation Energy. *J. Chem. Phys.*
639 **1975**, *62*, 3835–3836.
- 640 (65) Andlauer, B.; Ottinger, C. Unimolecular Ion Decompositions:
641 Dependence of Rate Constants on Energy from Charge Exchange
642 Experiments. *J. Chem. Phys.* **1971**, *55*, 1471–1472.
- 643 (66) Field, F. H.; Hamlet, P.; Libby, W. F. Chemical Ionization Mass
644 Spectrometry. VII. Reactions of Benzene Ions with Benzene. *J. Am.*
645 *Chem. Soc.* **1967**, *89*, 6035–6038.
- 646 (67) Smith, R. D.; DeCorpo, J. J. A Study of the Mechanism of (2p)
647 Carbon Ion Reactions with Benzene at 1.0 to 12 Ev. *J. Chem. Phys.*
648 **1976**, *80*, 2904–2910.
- 649 (68) Ausloos, P. Structure of $C_4H_4^+$ Produced in the Unimolecular
650 Fragmentation of $C_6H_6^+$ and $C_5H_5^+$. *J. Am. Chem. Soc.* **1981**, *103*,
651 3931–3932.
- 652 (69) Krailler, R. E.; Russell, D. H.; Jarrold, M. F.; Bowers, M. T. Laser
653 Beam-Ion Beam Photodissociation Studies of $C_6H_6^+$ Radical Cations:
654 The 2,4-Hexadiyne System. *J. Am. Chem. Soc.* **1985**, *107*, 2346–2354.
- 655 (70) Boechar-Roberty, H. M.; Neves, R.; Pilling, S.; Lago, A. F.; de
656 Souza, G. G. B. Dissociation of the Benzene Molecule by UV and Soft
657 X-Rays in Circumstellar Environment. *Mon. Not. R. Astron. Soc.* **2005**,
658 *000*, 1–8.
- 659 (71) Newby, J. J.; Stearns, J. A.; Liu, C.-P.; Zwier, T. S.
660 Photochemical and Discharge-Driven Pathways to Aromatic Products
661 from 1,3-Butadiene. *J. Phys. Chem. A* **2007**, *111*, 10914–10927.
- 662 (72) Ma, L.; Takashima, T.; Koka, J.; Kimber, H. J.; Cox, H.; Stace, A.
663 J. Conformation-Resolved UV Spectra of Pb(II) Complexes: A Gas
664 Phase Study of the Sandwich Structures $[Pb(Toluene)_2]^{2+}$ and
665 $[Pb(Benzene)_2]^{2+}$. *J. Chem. Phys.* **2013**, *138*, 164301/1–164301/11.
- 666 (73) Craciun, S.; Donald, K. J. Radical Bonding: Structure and
667 Stability of Bis(Phenalenyl) Complexes of Divalent Metals from across
668 the Periodic Table. *Inorg. Chem. (Washington, DC, U.S.)* **2009**, *48*,
669 5810–5819.
- 670 (74) Duncan, M. A. Structures, Energetics and Spectroscopy of Gas
671 Phase Transition Metal Ion-Benzene Complexes. *Int. J. Mass Spectrom.*
672 **2008**, *272*, 99–118.
- 673 (75) Deeth, R. J.; Gerloch, M. Redirected Ligand-Field Analysis. 2.
674 Asymmetric Chelation in Trigonal-Bipyramidal Copper(II) Com-
675 plexes. *Inorg. Chem.* **1984**, *23*, 3853–3861.
- 676 (76) Garcia-Fernandez, P.; Bersuker, I. B.; Boggs, J. E. Why Are
677 Some M12Molecules (M = Ca, Sr, Ba; L = H, F, Cl, Br) Bent While
678 Others Are Linear? Implications of the Pseudo Jahn-Teller Effect. *J.*
679 *Phys. Chem. A* **2007**, *111*, 10409–10415.
- 680 (77) Ipatov, A.; Cordova, F.; Doriol, L. J.; Casida, M. E. Excited-State
681 Spin-Contamination in Time-Dependent Density-Functional Theory
682 for Molecules with Open-Shell Ground States. *J. Mol. Struct.: THEOCHEM* **2009**, *914*, 60–73.